Syddansk Universitet

Optical properties of CDOM across the Polar Front in the Barents Sea

Hancke, Kasper; Hovland, Erlend K. ; Volent, Zsolt; Pettersen, Ragnhild; Johnsen, Geir; Moline, Mark; Sakshaug, Egil

Optical properties of CDOM across the Polar Front in the Barents Sea: Origin, distribution and significance

Kasper Hancke [a],[*],[1], Erlend K. Hovland [a], Zsolt Volent [b], Ragnhild Pettersen [a], Geir Johnsen [a],[c], Mark Moline [d], Egil Sakshaug [a]

[a] Norwegian University of Science and Technology, Department of Biology, Trondheim Biological Station, NTNU, N-7491 Trondheim, Norway
[b] SINTEF Fisheries and Aquaculture, N-7465 Trondheim, Norway
[c] University Centre on Svalbard, Pb 156, N-9171 Longyearbyen, Norway
[d] Biological Sciences Department, Center for Coastal Marine Sciences, Cal Poly, San Luis Obispo, CA 93407, USA

ARTICLE INFO

ABSTRACT

Colored Dissolved Organic Matter (CDOM) is an important optical constituent in seawater, which significantly attenuates the violet to blue portion of visible light. Thus, CDOM reduces the radiation energy available to phytoplankton and affects remote-sensing signals. We present data from two cruises transecting the Polar Front from Atlantic to Arctic waters in the Barents Sea, in 2007 and 2008. The latter took place during the spring bloom of phytoplankton in May ($0.2 < $[Chl a]$ < 13$ mg m^{-3}) and the former during August (max. [Chl a]$ < 2$ mg m^{-3}). Absorption by CDOM at 443 nm ranged from 0.004 to 0.080 m^{-1} during May and from 0.006 to 0.162 m^{-1} during August. Surprisingly, CDOM absorption differed little across the Polar Front, but was higher during August than during May ($P < 0.05$). The slope coefficient of the absorption spectra (S) ranged from 0.008 to 0.036 nm^{-1} (mean $= 0.015$ nm^{-1}) including both cruises, and varied little across the Front ($P > 0.05$). The CDOM remote sensing product from GlobColour correlated well with sampled data ($R^2 = 0.73$) during May. However, during August the satellite product performed poorly ($R^2 = 0.02$) due to extensive scattering caused by coccolithophorids in the Atlantic Water. The CDOM pool was of autochthonous (marine) origin as characterized from its S $vs.$ absorption relationship. Modeling showed that CDOM, on average, contributed equally to the light absorption as did phytoplankton (at 1 mg Chl a m^{-3}), and thereby reduces the amount of light available for primary production.

© 2012 Elsevier B.V. All rights reserved.

1. Introduction

The colored (chromophoric) fraction of the dissolved organic matter pool (CDOM, also known as 'yellow substance' or 'gilvin') can be an optically important constituent in ocean waters as it absorbs light, especially in the UV range of the visible spectrum (e.g. Bricaud et al., 1981; Jerlov, 1976; Nelson et al., 1998). The light absorption by the CDOM pool is usually defined as the absorption of light in a 0.2 μm pre-filtered seawater sample (Blough and Del Vecchio, 2002).

The CDOM absorption spectra $a_{CDOM}(\lambda)$ (m^{-1}) is commonly modeled as exponentially decreasing with increasing wavelength (Bricaud et al., 1981), i.e.

$$a_{cDOM}(\lambda) = a_{cDOM}(\lambda_0)e^{-S(\lambda-\lambda_0)} \tag{1}$$

where λ_0 is a reference wavelength for the model (350 nm in the present study) and S (nm^{-1}) is the slope coefficient, which characterizes the exponential decrease of light absorption with increasing wavelength (Bricaud et al., 1981). The CDOM concentration is given as absorption at a specific wavelength, e.g. $a_{CDOM}(443)$, while the slope coefficient describes the "signature" that reflects the chemical composition of the CDOM. As such, Carder et al. (1989) demonstrated that in the Gulf of Mexico, variations in S could be explained by the relative proportions of fulvic to humic acids in water samples.

Heterotrophic degradation of organic material is the primary source of marine-derived CDOM; while photomineralization and photobleaching are usually considered the main sinks (Blough and Del Vecchio, 2002; Mopper and Kieber, 2002; Sturluson et al., 2008). However, recent studies emphasize the complexity of the synthesis and degradation of CDOM in the Arctic and the apparent implications for the water column light attenuation, light availability to phytoplankton, and the biogeochemical turnover of organic matter, given the climatic changes and shrinking ice cover (Osburn et al., 2009; Stedmon et al., 2011).

In the Arctic region CDOM usually originates from marine phytoplankton (autochthonous) or terrestrial plants (allochthonous) through

* Corresponding author. Tel.: +45 6550 2724; fax: +45 6550 2786.
  E-mail address: khancke@biology.sdu.dk (K. Hancke).
[1] Present address: University of Southern Denmark, Institute of Biology and Nordic Center for Earth Evolution (NordCEE), Campusvej 55, DK-5230, Odense M, Denmark.

freshwater discharge from land (Gueguen et al., 2007; Kivimae et al., 2010; Osburn et al., 2009). In marine environments autochthonous CDOM can be discriminated from allochthonous CDOM by the slope coefficient S and its relationship to $a_{CDOM}(\lambda)$ in a given water mass (Stedmon and Markager, 2001). Stedmon et al. (2010) have recently shown that it is possible to quantify the mixing of water masses using CDOM signatures in near coastal waters.

Light absorption by CDOM reduces light availability for phytoplankton and shifts water-leaving radiance from blue towards the green and red wavelengths. Thus, CDOM, in addition to particulate matter, influences and structures the euphotic zones of the Arctic shelf seas with implications for the primary production (Osburn et al., 2009). Also, by absorbing more radiation in the upper layers of the sea, CDOM influences the forming of a stable upper mixed layer through heat trapping (Granskog et al., 2007). In order to accurately model these effects, a rigorous understanding of CDOM dynamics and abundance is needed.

Semi-analytical (SA) ocean color models, such as the Garver–Siegel–Maritorena model version 1 (GSM01) (Garver and Siegel, 1997; Maritorena et al., 2002) extract estimates of phytoplankton absorption (a_{ph}), $a_{CDOM}(443)$, and particulate backscattering from water-leaving radiance. Since the absorption spectra of CDOM and phytoplankton overlap, the SA models are constrained with certain empirically determined parameters; in the case of GSM01 the spectral shape of a_{ph}, and the CDOM S-coefficient are considered constants. Global CDOM pattern studies, such as Siegel et al. (2002), are dependent on good satellite-based CDOM retrievals. Therefore, regional satellite data validation and investigations of CDOM variability are necessary.

The objective of the present study was to characterize the optical properties of CDOM in the Central Barents Sea, analyze the distribution of CDOM across the Polar Front and assess the origin of the CDOM pool in the Barents Sea. Furthermore, the study addresses the importance of the Barents Sea CDOM pool for the water column light attenuation and the light availability for phytoplankton photosynthesis, and evaluates the remote sensing application.

2. Methods

2.1. Study site, CTD and sample collection

Two cruises were undertaken in the central Barents Sea during August 2007 and May 2008 respectively, as part of the International Polar Year (IPY) program and the project Norwegian component of the Ecosystem Studies of Subarctic and Arctic Regions (NESSAR). From these cruises, 26 stations were included in the present study (14 stations in 2007 and 12 stations in 2008) sampled on both sides of the oceanic Polar Front, representing both Atlantic and Arctic waters, as well as mixtures of the two, i.e. the Frontal Water (Fig. 1). In situ profiles of conductivity, temperature, depth (CTD) and Chlorophyll a (Chl a) fluorescence at each station were measured using a Sea-Bird CTD (SBE9 system, Sea-Bird Electronic, US) equipped with a Seapoint fluorometer (Chlorophyll Fluorometer, Seapoint Sensors, US). Water from 3 to 7 depths were collected at each station for analyses of Total Chlorophyll a (denotes Chl a, chlorophyllide a, phaeophytin a and phaeophobide a) and CDOM, using Niskin bottles (5 L, model 1010C). A total of 342 discrete water samples (114 sampled triplicates) were analysed for TChl a and CDOM from the euphotic zone at depths between 1 and 80 m. TChl a was measured from GF/F filters extracted in 90% acetone without correction for phaeopigments. Analyses were performed fluorometrically (Holm-Hansen et al., 1965) using a (Turner Designs-10 fluorometer) at the Institute of Marine Research (www.imr.no).

2.2. CDOM sampling, storage and freezing experiment

Samples for CDOM analyses were filtered through 0.2 μm Minisart syringe filters, which had been prewashed with a minimum of 10 mL of sample, and stored at 4 °C in the dark in 50 mL sterile, high mechanical and chemical resistant polypropylene containers (Greiner Oio-One International). The samples from 2008 were analyzed onboard the research vessel within a couple of hours after sampling. Samples from 2007 were frozen (−20 °C) within an hour after filtration and analyzed approximately 3 months after sampling in the
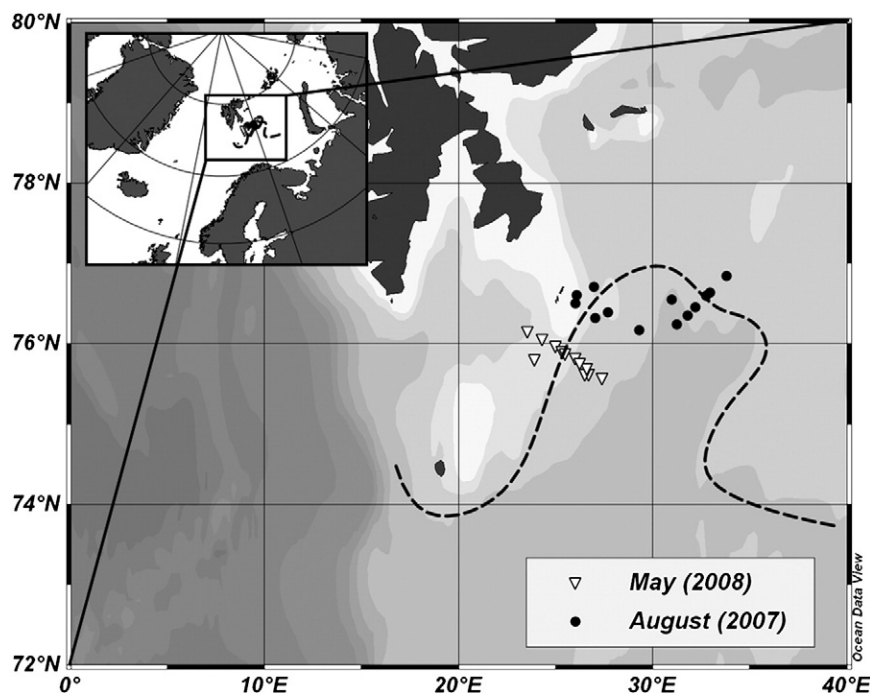

Fig. 1. Map of sampled stations during two cruises in the Central Barents Sea. The samples were collected during May 2008 (open triangles) and August 2007 (filled circles).The approximate position of the Polar Front during sampling is included (dashed line).

laboratory at Trondheim Biological Station (Trondheim, Norway). The frozen samples were slowly thawed to room temperature prior to analysis to match the temperature of the reference. This is important as the absorption of pure water is temperature dependent at red and near infrared wavelengths (Pegau and Zaneveld, 1993).

In order to test if the preservation by freezing of CDOM samples had an effect on the absorption properties we performed a laboratory experiment. A water sample of 5 L was collected from the Trondheimsfjord, Norway at 0.5 m depth (sal = 32.5, temp = 13 °C) from which 30 subsamples of 50 mL each (filtered through 0.2 μm Minisart syringe filters) were collected and stored in polypropylene containers. Three subsamples were analyzed immediately using a spectrophotometer while the remaining samples were frozen (−20 °C). Subsequently, triplicate samples were slowly thawed in the laboratory where after absorption was measured in the spectrophotometer at days 1, 2, 5, 8, 20, 94 and 120 after freezing (method in Section 2.3). The absorption coefficient $a_{CDOM}(350)$ is independent of the time that the samples were frozen (Probability (P) = 0.86), having an average value of 0.40 ± 0.03 (mean ± S.D. Fig 2.). The slope coefficient S also showed to be independent of the time samples were frozen (P = 0.63), having an average value of 0.015 ± 0.002 (mean ± S.D.). Thus, we concluded that preservation by freezing of CDOM samples (<4 months) prior to analyses had no significant effect on the estimation of $a_{CDOM}(350)$ nor on the slope coefficient S. In addition, the experiment showed that the uncertainty in determining the coefficients for $a_{CDOM}(350)$ and S was <1% (Fig. 2).
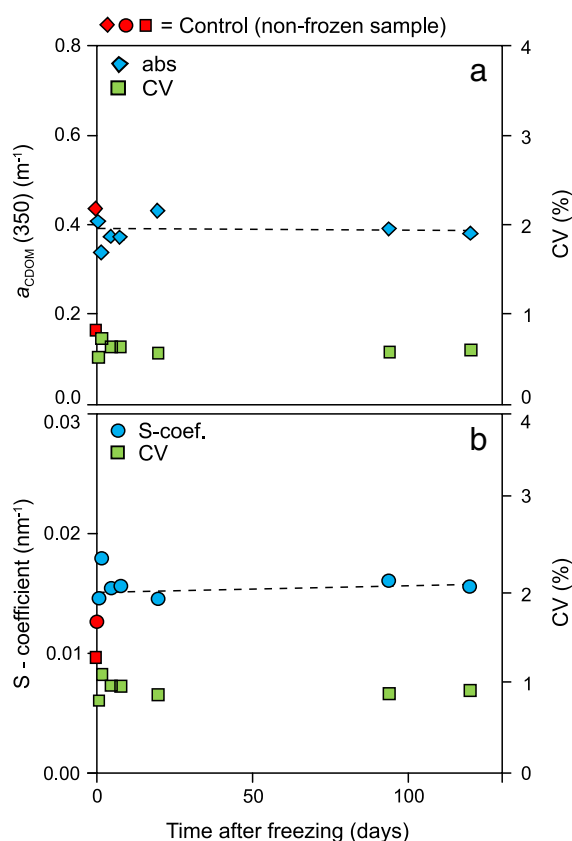
Fig. 2. Effects of the freezing experiment on CDOM samples on a) the $a_{CDOM}(350)$ and b) the S-coefficient. A set of CDOM samples with identical origin were frozen (−20 °C, n = 21) at t = 0 and subsequently stored for 1 to 120 days in the freezer. Frozen samples were thawed over a couple of hours to room temperature before measured in a spectrophotometer and compared to the non-frozen samples (control). Linear regression lines are included (dashed lines), showing no significant slope with time (i.e. a slope coefficient of one, P>0.05). CV (n = 3) is plotted on a secondary y-axes for both $a_{CDOM}(350)$ and S. A color version of this figure is available online.

2.3. Optical measurements

The optical density (OD_λ, dimensionless) of CDOM was measured in 10 cm quartz cuvettes over the 300–800 nm range with 2 nm increments using Milli-Q water as reference. A baseline correction was applied by subtracting the average absorbance from 690 to 700 nm to remove instrument baseline drift and scattering. In this range, absorption by CDOM is negligible as are effects of temperature and salinity on the absorbance of water (Mitchell et al., 2002). Samples were analyzed in a dual-beam spectrophotometer (Unicam 500 UV-Visible, Thermo-Spectronic, US). The absorption coefficient ($a_{CDOM}(\lambda)$, m^{-1}) were obtained from the equation

$$a_{cDOM}(\lambda) = 2.303 \cdot OD_\lambda / L, \qquad (2)$$

with L being the optical path length (in meters).

The absorption spectra were modeled from 350 to 550 nm according to Eq. (1) and the spectral slope coefficient (S, nm^{-1}) and aCDOM(λ) at specific wavelengths were determined for each sample using a non-linear regression routine in SigmaPlot 11.0 (SYSTAT Software Inc., San Jose, CA, USA). This routine was recommended to be superior to non-linear fitting routines (e.g. Matsuoka et al., 2011; Stedmon et al., 2000). The range for modeling the spectra was adopted because it represents a spectral range with sufficiently high signal for reliable estimation of the absorption properties and excludes wavebands with low signal-to-noise ratios caused by low absorption coefficients (>550 nm) as recommended by Babin et al. (2003), and also used in the literature for comparison (e.g. Matsuoka et al., 2011). See, in addition, Stedmon et al. (2000), Babin et al. (2003) and Granskog et al. (2007) for discussions on the modeling of CDOM spectra and log-transformed linear vs. non-linear fitting routines for CDOM spectra.

2.4. Remotely sensed data collection

Remotely sensed data of the CDOM absorption at 443 nm were downloaded at 4.6 km resolution from the GlobColour database (merged SeaWiFS, MODIS/AQUA and MERIS data) for both the 2007 and 2008 cruise periods, and analyzed with the BEAM software package in VISAT (Brockmann Consult, ver. 4.7). All images were sinusoidally reprojected at the 30° meridian with the 'nearest neighbor' recalculation method, before exporting the CDOM absorption values as 3×3 pixels surrounding each in situ station. The mean of the 3×3 pixel values was calculated from the image that was closest in time (<2 days) to a given station, and that yielded at least one valid pixel.

3. Results

3.1. Hydrographic conditions

A total of 25 stations were sampled in the Central Barents Sea across the Polar Front, 12 stations in May 2008 and 13 stations in August 2007 (Fig. 1). The study area contained two major water masses, i.e. Atlantic Water dominating to the south of the Polar Front and Arctic Water dominating to the north of the Polar Front. The Polar Front was characterized by relatively strong horizontal gradients in temperature and salinity but weak density gradients because of density compensation (Fer and Drinkwater, this issue; Våge et al., this issue). Atlantic Water was characterized as having salinities near or above 34.9 consisting with the classical definition by (Carmack, 1990; Loeng, 1991), and having temperatures between 1 and 7 °C (Fig. 3). Arctic Water was characterized having salinities <34.8 and, in most cases, having temperatures below 1 °C (Loeng, 1991). The high water temperatures at some of the Arctic stations measured during August 2007 (Fig. 3b) were caused by solar heating of the surface
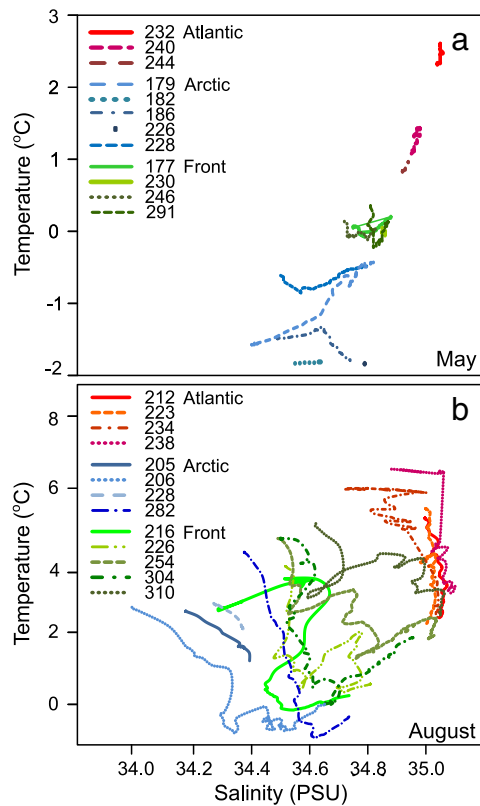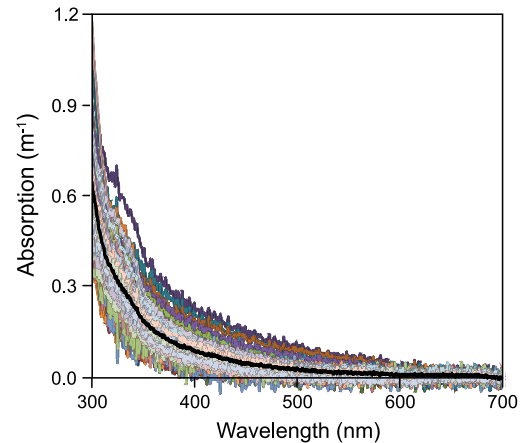
Fig. 3. The potential temperature *vs.* salinity for sampled stations during a) May 2008 and b) August 2007. The categorization of stations into Atlantic, Arctic and Frontal waters were done according to their T-S properties, as shown.

Fig. 4. Measured absorption spectra of all CDOM samples from the Barents Sea during May 2008 and August 2007. The thick black line represents the average absorption spectrum. A color version of this figure is available online.

water and as such were excluded when characterizing the water type. The region between the Atlantic and Arctic waters were characterized as Frontal Water representing a mixture of the two water masses and having intermediate temperature and salinity properties relative to the Atlantic and Arctic waters. All stations, as well as each water sample, were characterized as representing either Atlantic, Arctic or Frontal waters, respectively, depending on the hydrographic conditions at the sampled station as described above (Fig. 3).

3.2. Physical and optical properties in August 2007

During the cruise in August the physical and biological properties of the investigated waters, at both sides of the Polar Front, were characterized as typical late summer post-bloom conditions. TChl *a* concentrations were generally low (<1.0 mg m^{-3}, ranging from 0.12 to 2.8 mg m^{-3}), with the highest concentrations observed at the Atlantic side of the Front (Table 1). At the time of sampling, a coccolithophorid bloom dominated the Atlantic water stations with the highest TChl *a* concentrations, which ranged from 1.0 and 2.8 mg m^{-3} in the euphotic zone (Hovland et al., 2012). There was no indication of higher TChl *a* concentrations inside the Front relative to the adjacent waters. Details of the hydrographic conditions and frontal features during the cruise are found in Våge et al. (this issue). For general descriptions of the physical oceanography for the Barents Sea see, e.g. Loeng (1991); (Loeng and Drinkwater, 2007).

The absorption by CDOM, $a_{CDOM}(443)$, ranged from 0.006 to 0.162 m^{-1} including both Atlantic, Arctic and Frontal waters, with an average of 0.062 ± 0.034 S.D (Table 1). All measured absorption spectra from the entire study are shown to visualize the average $a_{CDOM}(\lambda)$ and the corresponding range of absorption from 300 to 700 nm (Fig. 4). Testing the difference in $a_{CDOM}(443)$ between the three investigated waters showed a statistically significant difference as tested using a One Way ANOVA test (P<0.05, Kruskal–Wallis test). A pairwise Multiple Comparison Procedure (Dunn's method) was then used to identify a slightly but significantly lower $a_{CDOM}(443)$ from the Arctic Water than compared to the Atlantic and Frontal waters (P<0.05). There was no statistically significant difference (P>0.05) of $a_{CDOM}(443)$ between the Atlantic and Frontal waters. The slope coefficient, S, ranged from 0.008 and 0.027 nm^{-1} with an average of 0.014 ± 0.004 S.D (Table 1). There was no statistically significant difference (P>0.05) in S between the three investigated waters.

Table 1
CDOM optical properties and TChl *a* sampled in May 2008 and August 2007. Numbers are average ± SD. To facilitate comparison with previously published data both aCDOM(350) and aCDOM(443) is shown. Values were computed from modeled CDOM absorption spectra (*n*, Eq. (1)) from triplicated measurements.

	Water mass	*n*	$a_{cDOM}(350)$, m^{-1}	$a_{cDOM}(443)$, m^{-1}	S, nm^{-1}	TChl *a*, mg m^{-3}
May 2008, spring development						
	Atlantic	9	0.14 ± 0.02	0.035 ± 0.013	0.015 ± 0.003	1.3 ± 1.1
	Arctic	17	0.17 ± 0.03	0.046 ± 0.016	0.014 ± 0.002	5.0 ± 4.7
	Frontal	11	0.17 ± 0.05	0.040 ± 0.023	0.018 ± 0.007	3.6 ± 4.8
	Total/Average for 2008	37	0.16 ± 0.04	0.041 ± 0.018	0.016 ± 0.004	3.7 ± 4.2
August 2007, late-summer						
	Atlantic	24	0.24 ± 0.07	0.084 ± 0.037	0.013 ± 0.003	1.05 ± 0.79
	Arctic	20	0.14 ± 0.06	0.039 ± 0.030	0.017 ± 0.005	0.58 ± 0.37
	Frontal	27	0.19 ± 0.04	0.060 ± 0.022	0.013 ± 0.003	0.44 ± 0.21
	Total/Average for 2007	71	0.20 ± 0.07	0.062 ± 0.034	0.014 ± 0.004	0.70 ± 0.58
Entire dataset	Total/Average	108	0.18 ± 0.06	0.055 ± 0.031	0.015 ± 0.005	1.8 ± 2.9

3.3. Physical and optical properties in May 2008

The May cruise was carried out during the early growing period of the phytoplankton bloom in the Barents Sea. In the Arctic Water the bloom period had presumably just begun prior to visiting the stations based on the weak stratification of the water column and the relatively high TChl a concentrations in the surface layers, 0.2 to 13.2 mg m^{-3} (Table 1). From sea-ice data (www.met.no), it was concluded that the sea ice had broken up approximately a week prior to sampling. In the Atlantic Water the TChl a concentration ranged from 0.2 to 3.4 mg m^{-3} (Table 1). The Frontal region represented a mixture of the Atlantic and the Arctic waters regarding both the physical and biological properties. Details of the hydrographic conditions and frontal features during the cruise are given in (Fer and Drinkwater, this issue).

In May the $a_{CDOM}(443)$ ranged from 0.004 to 0.080 m^{-1} including both Atlantic, Arctic and Frontal waters, with an average of 0.041 $\pm$ 0.018 S.D (Table 1, Fig. 4). There was no statistically significant difference in a$_{CDOM}(443)$ between the three sampled waters, i.e. Atlantic, Arctic and Frontal (P>0.05, Kruskal–Wallis One Way ANOVA). The S-coefficient ranged from 0.011 to 0.036 nm^{-1} with an average of 0.016 $\pm$ 0.004 S.D (Table 1). There was no statistically significant difference (P>0.05) of S between the three investigated waters.

3.4. Inter annual variability of absorption properties

The $a_{CDOM}(443)$ was on average higher (~50%) in August 2007 than in May 2008 (Table 1). In addition, the standard deviation of $a_{CDOM}(443)$ was ~2-fold higher during August than in May. The difference in $a_{CDOM}(443)$ between May and August was statistically significant (P = 0.006, Mann–Whitney Rank Sum test of variance), and

was primarily related to the seasonal differences in Atlantic Water rather than in Arctic and Frontal waters (Table 1, Fig. 5).

The S coefficients differed only slightly between May and August (Table 1), albeit significantly (P<0.05, Mann–Whitney Rank Sum test of variance).

3.5. Relationship of absorption properties to TChl a and salinity

In our study, there was no apparent relationship between $a_{CDOM}(443)$ and TChl a (Fig. 5a). As stated above, the TChl a concentration varied ~2 fold, being higher during May than August, while $a_{CDOM}(443)$ on average was higher during August than during May. Analyzing the entire dataset we found no correlation between $a_{CDOM}(443)$ and TChl a for any of the investigated waters (Fig. 5a). This applied to May and August separately as well (data not shown) indicating that a$_{CDOM}(443)$ and TChl a were independent across seasons and growth conditions. Similarly, no apparent relationship was observed between S and TChl a (Fig. 5b).

In order to relate the CDOM absorption properties to the different waters across the Polar Front, $a_{CDOM}(443)$ and S coefficients were compared to salinity (Fig. 6). These analyses revealed no significant relationship between $a_{CDOM}(443)$ and salinity (Fig. 6a), nor between S and salinity (Fig. 6b), either between or within the different waters.

3.6. Remotely sensed vs. in situ CDOM absorption properties

Remotely sensed data of the CDOM absorption at 443 nm were analyzed and compared to in situ sampled data in order to evaluate the GSM01 remotely sensed product from the GlobColour database (Garver and Siegel, 1997; Maritorena et al., 2002) for the Central Barents Sea. From the comparison, we observed a strong significant correlation (slope coefficient = 1.1, R^2 = 0.73, P = 0.015) between the
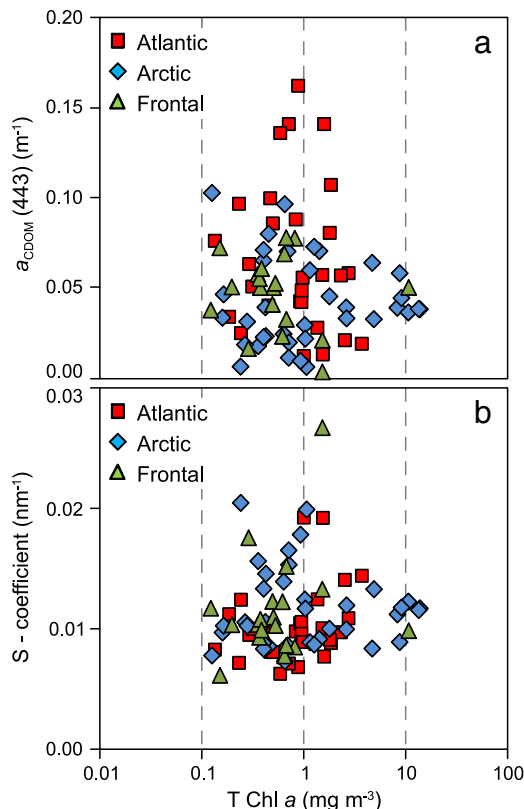
Fig. 5. The distribution of a) $a_{CDOM}(443)$ and b) S as a function of TChl a (note x on log$_{10}$ scale). No obvious relationship were observed of $a_{CDOM}(443)$ or S vs. TChl a in neither Atlantic (red squares), Arctic (blue diamonds), nor Frontal (green triangles) waters. A color version of this figure is available online.
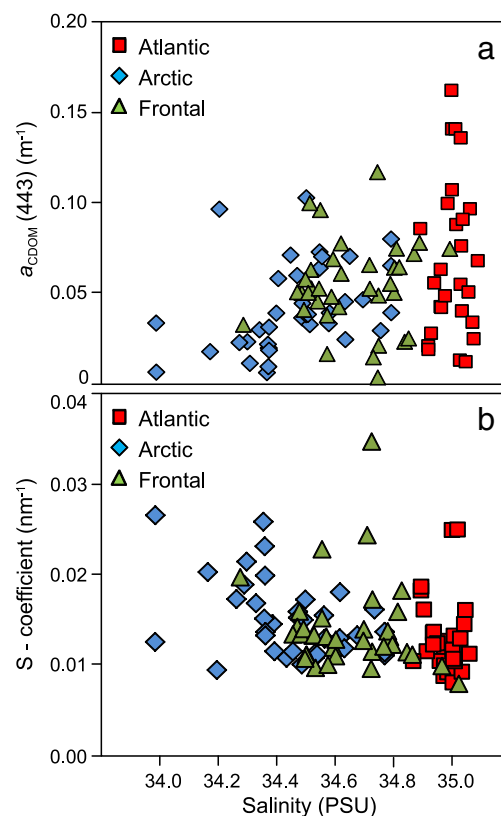
Fig. 6. The distribution of a) $a_{CDOM}(443)$ and b) S as a function of salinity. No obvious relationship were observed of $a_{CDOM}(443)$ and S vs. salinity. Symbols as in Fig. 4. A color version of this figure is available online.
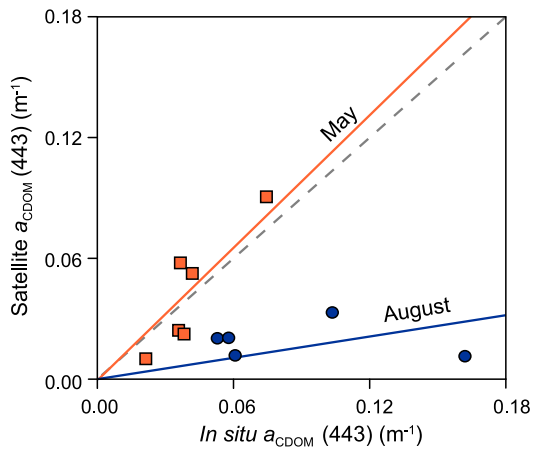
Fig. 7. Comparing $a_{CDOM}(443)$ from *in situ* collected samples *vs.* remotely sensed data. Samples were collected during a diatom-dominated spring bloom in May (2008), and during a coccolithophorid-dominated bloom in August (2007). Linear fits to the 'May' and 'August' had slope coefficients of 1.10 ($R^2 = 0.73$) and 0.18 ($R^2 = 0.02$), respectively. The grey dashed line represents the optimum one-to-one line. A color version of this figure is available online.

in situ and the GlobColour-merged satellite data for $a_{CDOM}(443)$ during the spring bloom in May 2008, when the water column was dominated by large diatoms (Fig. 7). During the late-summer conditions in August 2007, however, there was no apparent relationship between the GlobColour product and *in situ* observations (slope = 0.18, $R^2 = 0.02$, Fig. 7).

4. Discussion

The sampled characteristics of the CDOM absorption, $a_{CDOM}(\lambda)$ and slope coefficient, S, in the Barents Sea (Figs. 4 to 6, Table 1) fell within the range of previously published data from the Barents Sea (Aas et al., 2002), the Greenland Sea (Stedmon and Markager, 2001) and the Central Arctic surface waters (Pegau, 2002). In a pan-arctic perspective, similar or higher values of $a_{CDOM}(\lambda)$ have been reported from the Hudson Strait and Foxe Channel in the Canadian Arctic (Granskog et al., 2007), from the Western Arctic Ocean Shelf (Gueguen et al., 2005), and the Chukchi Sea (Hill, 2008), all of which however, report influence of CDOM from river export. Compared to non-arctic regions, the observed CDOM absorption in the Barents Sea fell within the range of values reported from the Mediterranean and Atlantic Ocean (Babin et al., 2003). The observed values for S fell within the range of previously published data from the Barents Sea, the Greenland Sea and Arctic Ocean (Aas et al., 2002; Pegau, 2002; Stedmon and Markager, 2001). Higher values of S have been reported from coastal regions with substantial input of terrestrial CDOM from river runoffs, for instance of the coast of Canada and Alaska (Granskog et al., 2007; Matsuoka et al., 2011). Of general consideration, S has typically been reported in the range from 0.010 to 0.022 in marine open water systems (Kirkpatrick et al., 2003), while in coastal and freshwaters systems S can be much greater (e.g. Blough and Vecchio, 2002). It is important to note that S often is calculated using different wavebands of the CDOM absorption spectrum in the scientific literature with potential effects on the modeled S values, e.g. (Pegau, 2002) used 400 to 700 nm, (Stedmon and Markager, 2001) 300 to 600 nm, and (Matsuoka et al., 2011) 350 to 500 nm. The consequence of this is discussed further in subsection 4.2.

4.1. CDOM absorption and distribution across the Polar Front

An important component of this study was to evaluate the distribution of CDOM across the Polar Front in the Central Barents Sea. In general, frontal systems often are associated with an enhanced

primary production that subsequently leads to enhanced microbial and biogeochemical activity (Claustre et al., 2000). Thus, we initially expected to find an increased biological activity and elevated $a_{CDOM}(\lambda)$ inside the Polar Frontal waters compared to the adjacent Atlantic and Arctic waters. Such a scenario would compare favorably with other frontal regions where CDOM accumulates and enhanced microbial activity has been reported, both tracers for enhanced biological production and activity (e.g. Claustre et al., 2000). Surprisingly, in the present study we did not observe any significant increase in $a_{CDOM}(443)$ in the waters within the Polar Front compared to the adjacent waters (Figs. 5 and 6, Table 1). This applied to both to the spring bloom in May 2008 and late summer in August 2007. We thus concluded that from $a_{CDOM}(\lambda)$, it was not possible to identify any increased biological activity associated with the Polar Front as a physical feature. Nor did the TChl *a* distribution indicate increased activity within the Front (Fig. 5, Table 1). This is consistent with a lack of enhanced biological activity as revealed by fluorescence measurements (Fer and Drinkwater, this issue), bacteria (Yngve Børsheim, personal communication, Institute of Marine Research, Bergen, Norway), and Fast Repetition Rate Fluorometry (Svein Rune Erga, personal communication, University of Bergen, Norway).

Overall, little difference in $a_{CDOM}(443)$ was observed in the waters across the Polar Front and between seasons. The exception from this was the Arctic Water in August (2007) showing slightly but significantly lower $a_{CDOM}(443)$ than the Atlantic and Frontal from the same season ($P < 0.05$, Table 1). Seasonally, $a_{CDOM}(443)$ was, on average, higher during August than May ($P < 0.01$, Figs. 5 and 6, Table 1). The latter was primarily caused by the higher values of $a_{CDOM}(443)$ in the Atlantic Water but also the Frontal Water during August. The observations most likely demonstrate an accumulation of CDOM from biological activity over the course of the growth season, explaining the elevated $a_{CDOM}(443)$ values observed late in the season. In western Arctic waters a strong seasonal trend in both $aCDOM$ and S has been observed (Matsuoka et al., 2011). They found a significant increase of $a_{CDOM}(440)$ towards the end of the growth season, while S increased from spring to summer with a strong subsequent decrease from summer to autumn. They linked the seasonal dynamics of the optical properties of CDOM to the large amount of freshwater originating from the Yukon River. We suggest that the absence of a correlation between TChl *a* and $a_{CDOM}(443)$ in our data (Fig. 5) is likely explained by hysteresis; i.e. that high values for CDOM are remnants derived from blooms that were concluded days or weeks earlier. Therefore, while the analyzed correlation between TChl *a* and $a_{CDOM}(443)$ represents a comparison at time of sampling, it would be more meaningful if data on time integrated TChl *a* for the area were available to assess if CDOM in the Barents Sea represents the 'end product' of local primary production.

The relationships of $a_{CDOM}(443)$ and S with salinity were complex (Fig. 6). In coastal and shelf waters dominated by large river outputs, a negative correlation between CDOM absorption and salinity is often reported, as high CDOM concentrations of terrestrial origin in rivers are diluted as the river water mixes with sea water, e.g. as in the Hudson Bay/Strait (Granskog et al., 2007) and on the Western Arctic Shelf (Gueguen et al., 2007). Also, melting of sea ice in the Arctic can alter the CDOM absorption properties in both a positive and negative way. Melting of sea ice has been reported to dilute surface CDOM concentrations, but on the other hand it also adds to the CDOM pool from 'wash-out' of ice-associated biological production (Granskog et al., 2007; Pegau, 2002; Scully and Miller, 2000).

Based on the present data we suggest that riverine input did not influence the central Barents Sea, thus explaining the lack of correlation between salinity and $a_{CDOM}(\lambda)$. This is supported by the conclusion that the Barents Sea CDOM pool is of autochthonous origin (see Section 4.2). A lack of correlation between salinity and CDOM abundance in the region is additionally supported by observations from the northern part of the Barents Sea (Aas and Hokedal, 1996).

4.2. Origin of the CDOM pool in the Barents Sea

Stedmon and Markager (2001) published a model to distinguish between marine and terrestrial (autochthonous and allochthonous, respectively) CDOM based on data from the Greenland Sea and the North Sea. The model proposes an inverse relationship between $a_{CDOM}(375)$ and S for autochthonous CDOM (dashed line in Fig. 8). This relationship has also previously been reported (e.g. Nelson and Guarda, 1995; Vodacek et al., 1997). In our study, the distribution of the slope coefficient S as a function of $a_{CDOM}(375)$ demonstrated a robust relationship between the two parameters (Fig. 8). Applying the model by Stedmon and Markager (2001) to the present data set, it is evident that almost the entire data set from the present study fits well within the limits (dotted line in Fig. 8) for autochthonous CDOM. This shows that the CDOM pool across the Polar Front in the Barents Sea is of autochthonous origin.

In coastal water, with high terrestrial input, allochthonous CDOM often shows S as being independent of $a_{CDOM}(\lambda)$, typical with S-values of 0.015 to 0.025 nm^{-1} (Granskog et al., 2007; Gueguen et al., 2005; Stedmon and Markager, 2001). A comprehensive study of CDOM absorption properties of the European Coastal waters showed no relationship of $a_{CDOM}(443)$ *vs.* S, giving an average S of ~0.018 nm^{-1} (Babin et al., 2003).

There is an apparent contradiction in the lack of correlation between $a_{CDOM}(443)$ and TChl a, and the conclusion that CDOM in the Barents Sea is autochthonous. As suggested above, this can be explained by a temporal mismatch between the intensive spring bloom and the subsequent degradation of phytoplankton into detritus and CDOM. Also, due to the West Spitsbergen Current that intrudes the basin from the north (Lind and Ingvaldsen, 2012); the water north of the Polar Front in the Barents Sea is rarely 'pure' Arctic and may contain residues of CDOM produced in Atlantic Water.

The difference between the mean of the Stedmon and Markager (2001) model (dashed line, Fig. 8) and the calculated mean for the present data set (solid line, Fig. 8) is likely the result of slightly different calculation methods. The choice of waveband used to model S from the CDOM absorption spectra (Section 2.3) is known to influence the computed values for S (Babin et al., 2003; Granskog et al., 2007; Stedmon et al., 2000). This occurrence is a possible explanation for S being depressed by ~0.002 nm in the present study compared to the study by Stedmon and Markager (2001). We modeled CDOM absorption in the range of 350 to 550 nm whereas Stedmon and Markager (2001) modeled S in the waveband range from 300 to 650 nm. Recalculating S for the present data set in the 300 to 650 nm range resulted in an increase of S of ~0.002 nm, almost exactly accounting for the difference in the modeled mean between the two models in Fig. 8 (dashed and solid lines).

4.3. Significance of CDOM absorption to phytoplankton absorption in the Barents Sea

Traditionally, in open oceans as well as the Arctic Ocean, CDOM absorption has been considered of minor importance, with little or no annual variability (Nelson and Siegel, 2002). However, recent studies of optical properties have demonstrated differently, concluding that CDOM plays an important role for the light absorption in the surface waters (Granskog et al., 2007; Hill, 2008; Pegau, 2002; Stedmon et al., 2011), thereby reducing the light available for phytoplankton photosynthesis and primary productivity (Arrigo et al., 2011; Matsuoka et al., 2011). In addition, CDOM has been shown to contribute significantly to trapping of heat in the surface water with implications to the Arctic region through increased sea-ice melt, warming of the water column and stratification of the surface layer (Hill, 2008).

CDOM quantitatively competes with phytoplankton for light, as it absorbs heavily in the blue part in the Photosynthetic Active Radiation (PAR) band where phytoplankton light-harvesting pigments also absorb light most efficiently (Fig. 4). By comparing the average CDOM absorption spectrum found in the Barents Sea during our study with phytoplankton absorption (a representative *in situ*-derived phytoplankton absorption spectrum from the western Arctic by Matsuoka et al. (2011)), it is evident that light absorption by CDOM is relatively substantial (Fig. 9). When Chl a is below 1 mg m^{-3}, which is the case for most of the growth season in the Barents Sea following the decline in the spring bloom, CDOM absorbs light in the PAR region more efficiently than phytoplankton (Fig. 9). From modeling the underwater light attenuation with the presence of CDOM (average from this study) and phytoplankton [from (Matsuoka et al., 2011)] it is evident that CDOM contributes equally to the light attenuation (1.0 times) as do phytoplankton at 1 mg Chl a m^{-3}, and ~0.75 times at 5 mg Chl a m^{-3} (Fig. 9 and Table 2). These numbers were modeled by taking into the account the spectral attenuation properties integrating from 400 to 700 nm over the upper 10 meters of a water column consisting of
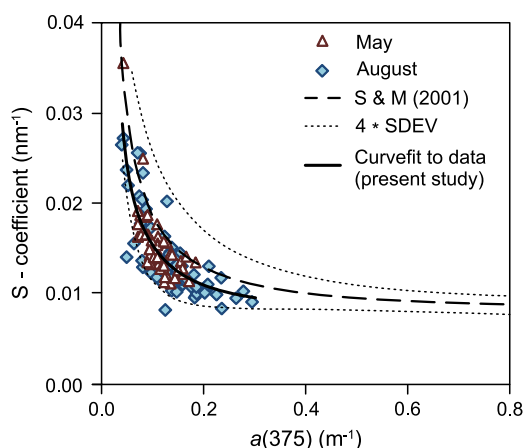
Fig. 8. The $a_{CDOM}(375)$ *vs.* S distribution for samples collected during May (triangles) and August (diamonds), respectively. Overlaid is a S-$a_{CDOM}(443)$ model (dashed line, S = 7.4 + 1.1/$a_{CDOM}(375)$) for autochthonous CDOM adopted from Stedmon and Markager (2001), with limits defined as ±4 standard deviations times the precision of the S-estimate (dotted lines). Data points that fall within the model limits are defined as of autochthonous origin. The solid line represents the modeled average for the present study data set. A color version of this figure is available online.
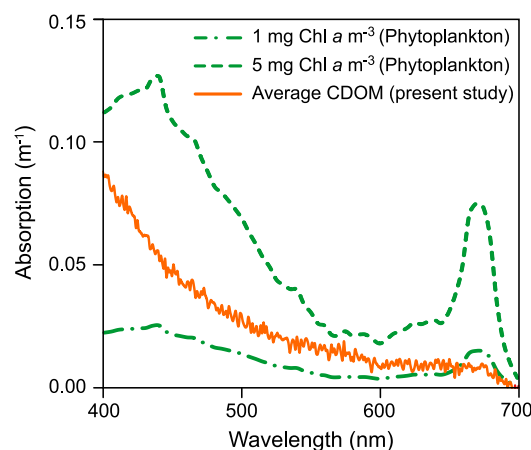
Fig. 9. The average modeled CDOM absorption spectrum (thick line from Fig. 3) together with representative averaged *in situ*-derived phytoplankton absorption spectra at concentration of 1 and 5 mg Chl a m^{-3}, from the western Arctic by Matsuoka et al. (2011). The figure illustrates the absolute absorption of light by CDOM in the Barents Sea in comparison with phytoplankton at two different concentrations. A color version of this figure is available online.

Table 2

Ratio of absorbed light in the upper 10 m of the water column and the 1% and 10% irradiance depths ($Z_{1\%}$, i.e. the euphotic zone, and $Z_{10\%}$) by pure water, CDOM and Chl a at two concentrations. CDOM and Chl a as in Fig. 9. Corresponding PAR attenuation (K_{d_PAR}, m^{-1}) in brackets. Pure water is from Pope and Fry (1997). Data are modeled using ECOLIGHT (C. Mobley, Sequoia, US) assuming a vertically homogeneous water column, using phytoplankton scattering from Loisel and Morel (1998), $b/bb = 0.014$, and constant sky and atmospheric condition and a sun angle relative to May 1st in the Central Barents Sea.

	Absorbed light at 10 m (relative to surface)	$Z_{10\%}$ (m)	$Z_{1\%}$ (m)
Pure water	0.60 (0.09)	70 (0.03)	235 (0.02)
CDOM *	0.73 (0.13)	22.4 (0.10)	55.5 (0.08)
1 mg Chl a m^{-3}	0.72 (0.13)	24.0 (0.09)	60.0 (0.08)
1 mg Chl a m^{-3} + CDOM	0.80 (0.16)	15.6 (0.15)	37.5 (0.12)
5 mg Chl a m^{-3} + CDOM	0.92 (0.26)	8.6 (0.26)	20.5 (0.23)

* Average concentration found in this study (Table 1).

pure water, water + CDOM, water + Chl a, and water + Chl a + CDOM, respectively, using a radiative transfer model (ECOLIGHT, C. Mobley, Sequoia, US). Also, CDOM, at the average concentration found in the Barents Sea, increased the light absorption by ~22% in the upper 10 m when compared to pure water (Table 2).

Hence, CDOM plays a major role for the light and heat absorption in the Barents Sea a large part of the year, with quantitative importance for the primary productivity and the stratification of the water column, as also supported in the literature (Arrigo et al., 2008; Granskog et al., 2007). In fact, Hill (2008) suggests that CDOM can be responsible for more than 30% of the trapping of light and heat in the Arctic. Similarly, Pegau (2002) found that CDOM increased the absorption of radiation between 350 and 700 nm by >30% in the top 10 m in the central Arctic compared to the clearest natural waters, a process that will stimulate the stratifying progression. The present study supports these findings and underlines the importance of the autochthonous CDOM for the underwater light absorption in the central Barents Sea, in contrast to the allochthonous CDOM abundant on the Canadian Arctic Shelf.

On a global perspective, Nelson and Siegel (2002) estimate that ~57% of the surface non-water absorption is due to CDOM, implying that with decreasing Chl a the contribution to absorption of CDOM and detritus increases. Furthermore, they note that at [Chl a] ~0.5 mg m^{-3} the absorption by CDOM and phytoplankton is approximately the same. At [Chl a] <0.5 mg m^{-3} CDOM absorption dominates the total absorption. Our findings suggest the CDOM absorption in the Barents Sea is equally important to phytoplankton absorption compared to lower latitude ecosystems and even more important in relation to the heat flux (as it influences the sea ice dynamics) than on average over the global ocean.

4.4. Remotely sensed vs. in situ CDOM absorption

The merged satellite data from GlobColour correlated well with *in situ* sampled data for the spring bloom in May 2008 (Fig. 7). However, during the late-summer bloom of August 2007, this correlation was weak, presumably due to the presence of coccolithophorids and free coccoliths in the water. There were high amounts of calcite in Atlantic waters within our study area in the late summer, easily visible as a green coloring of the water (Hovland et al., 2012). We did not have a data set to support rigorous testing of variables such as water types towards the satellite CDOM product performance, but this is clearly needed in further studies for verifying the application of remotely-sensed CDOM data in the Arctic region. This point is emphasized by recent literature reporting that CDOM greatly influences the water color measured by remote sensing techniques, which is used extensively to estimate phytoplankton productivity (Arrigo et al., 2008; Stedmon et al., 2011). Therefore, properties and distribution of CDOM in the Arctic need to be described and characterized carefully before remote sensing techniques and bio-optical models will be trustworthy for the Arctic

region (Alver et al., 2012). For now, remotely sensed CDOM products need to be used with caution during periods of abundant coccolithophorid presence, which have been annual events in the Barents Sea and the Arctic region over the last two decade (Hovland et al., 2012; Merico et al., 2003; Smyth et al., 2004).

5. Conclusions

Colored Dissolved Organic Matter (CDOM) is important for the light attenuation in the Central Barents Sea. Overall, we observed no or only little difference in $a_{CDOM}(\lambda)$ and S between the investigated Atlantic, Arctic and Frontal waters, leaving no indication of an elevated biological activity associated with the Polar Front. Nor did we observe a relationship of the CDOM absorption to TChl a and salinity across the Polar Front. Data suggest a seasonal trend of increasing $a_{CDOM}(\lambda)$ throughout the growth season, however, not influencing the curvature of the absorption spectra, S. The CDOM remote sensing product correlated well with sampled data during spring but the correlation was poor in late summer during a coccolithophorid bloom. The CDOM pool was concluded to be of autochthonous (marine) origin and important for the light availability to phytoplankton. CDOM contributed equally to the light attenuation of PAR as 1 mg Chl a integrated over the top 10 m (400 to 700 nm), comparing to a ~22% increase of attenuation relative to pure water. CDOM proved to be important to the underwater light climate and should be taken into account in bio-optical models and in remote sensing algorithms for the Arctic-Subarctic region.

References

Aas, E., Hokedal, J., 1996. Penetration of ultraviolet B, blue and quanta irradiance into Svalbard waters. Polar Res. 15, 127–138.

Aas, E., Høkedal, J., Højerslev, N.K., Sandvik, R., Sakshaug, E., 2002. Spectral properties and UV-attenuation in Arctic marine waters. In: Hessen, D.O. (Ed.), UV Radiation and Arctic Ecosystems. Springer-Verlag, Berlin Heidelberg.

Alver, M.O., Hancke, K., Slagstad, D., Sakshaug, E., 2012. A spectrally-resolved light propagation model for aquatic systems: Steps toward parameterizing primary production. J. Mar. Syst., http://dx.doi.org/10.1016/j.jmarsys.2012.03.007.

Arrigo, K.R., van Dijken, G., Pabi, S., 2008. Impact of a shrinking Arctic ice cover on marine primary production. Geophys. Res. Lett. 35.

Arrigo, K.R., Matrai, P.A., Van Dijken, G.L., 2011. Primary productivity in the Arctic Ocean: impacts of complex optical properties and subsurface chlorophyll maxima on large-scale estimates. J. Geophys. Res. 116, http://dx.doi.org/10.1029/2011JC007273.

Babin, M., Stramski, D., Ferrari, G.M., Claustre, H., Bricaud, A., Obolensky, G., Hoepffner, N., 2003. Variations in the light absorption coefficients of phytoplankton, nonalgal particles, and dissolved organic matter in coastal waters around Europe. J. Geophys. Res.-Oceans 108.

Blough, N.V., Del Vecchio, R., 2002. Chromophoric DOM in the coastal environment. In: Dennis, A.H., Craig, A.C. (Eds.), Biogeochemistry of Marine Dissolved Organic Matter. Academic Press, San Diego, pp. 509–546.

Blough, N.V., Vecchio, R.D., 2002. Chromophoric DOM in coastal environment. In: Hansell, D.A., Carlson, C.A. (Eds.), Biogeochemistry of Marine Dissolved Organic Matter. Elsevier Science, San Diego, pp. 509–546.

Bricaud, A., Morel, A., Prieur, L., 1981. Absorption by dissolved organic-matter of the sea (yellow substance) in the UV and visible domains. Limnol. Oceanogr. 26, 43–53.

Carder, K.L., Steward, R.G., Harvey, G.R., Ortner, P.B., 1989. Marine humic and fulvic-acids — their effects on remote-sensing of ocean chlorophyll. Limnol. Oceanogr. 34, 68–81.

Carmack, E., 1990. Large scale physical oceanography of polar oceans. In: Smith, W.O. (Ed.), Polar oceanography, Part A: Physical Science. Academic Press, New York, pp. 171–222.

Claustre, H., Fell, F., Oubelkheir, K., Prieur, L., Sciandra, A., Gentili, B., Babin, M., 2000. Continuous monitoring of surface optical properties across a geostrophic front: biogeochemical inferences. Limnol. Oceanogr. 45, 309–321.

Fer, I., Drinkwater, K., this issue. Mixing in the Barents Sea Polar Front near Hopen in spring. J. Mar. Syst.

Garver, S.A., Siegel, D.A., 1997. Inherent optical property inversion of ocean color spectra and its biogeochemical interpretation 1. Time series from the Sargasso Sea. J. Geophys. Res. 102, 18607–18625.

Granskog, M.A., Macdonald, R.W., Mundy, C.J., Barber, D.G., 2007. Distribution, characteristics and potential impacts of chromophoric dissolved organic matter (CDOM) in Hudson Strait and Hudson Bay, Canada. Cont. Shelf Res. 27, 2032–2050.

Gueguen, C., Guo, L.D., Tanaka, N., 2005. Distributions and characteristics of colored dissolved organic matter in the Western Arctic Ocean. Cont. Shelf Res. 25, 1195–1207.

Gueguen, C., Guo, L.D., Yamamoto-Kawai, M., Tanaka, N., 2007. Colored dissolved organic matter dynamics across the shelf-basin interface in the western Arctic Ocean. J. Geophys. Res.-Oceans 112.

Hill, V.J., 2008. Impacts of chromophoric dissolved organic material on surface ocean heating in the Chukchi Sea. J. Geophys. Res.-Oceans 113.

Holm-Hansen, O., Lorenzen, C.J., Holmes, R.W., Strickland, J.D.H., 1965. Fluorometric determination of chlarophyll. J. Cons. Int. Explor. Mer 30, 3–15.

Hovland, E.K., Hancke, K., Alver, M.O., Drinkwater, K., Høkedal, J., Johnsen, G., Moline, M., Sakshaug, E., 2012. Optical impact of an Emiliania huxleyi bloom in the frontal region of the Barents Sea. J. Mar. Syst, http://dx.doi.org/10.1016/j.jmarsys.2012.07.002.

Jerlov, N.G., 1976. Marine optics. Oceanography Series, 14. Elsevier, Amsterdam, pp. 1–231.

Kirkpatrick, G.J., Orrico, C., Moline, M.A., Oliver, M., Schofield, O.M., 2003. Continuous hyperspectral absorption measurements of colored dissolved organic material in aquatic systems. Appl. Opt. 42, 6564–6568.

Kivimae, C., Bellerby, R.G.J., Fransson, A., Reigstad, M., Johannessen, T., 2010. A carbon budget for the Barents Sea. Deep-Sea Res. I Oceanogr. Res. Pap. 57, 1532–1542.

Lind, S., Ingvaldsen, R.B., 2012. Variability and impacts of Atlantic Water entering the Barents Sea from the north. Deep Sea Res. Part I 62, 70–88.

Loeng, H., 1991. Features of the physical oceanographic conditions of the Barents Sea. Polar Res. 10, 5–18.

Loeng, H., Drinkwater, K., 2007. An overview of the ecosystems of the Barents and Norwegian Seas and their response to climate variability, pp. 2478–2500.

Loisel, H., Morel, A., 1998. Light scattering and chlorophyll concentration in case 1 waters: a reexamination. Limnol. Oceanogr. 43, 847–858.

Maritorena, S., Siegel, D.A., Peterson, A.R., 2002. Optimization of a semianalytical ocean color model for global-scale applications. Appl. Opt. 41, 2705–2714.

Matsuoka, A., Hill, V., Huot, Y., Babin, M., Bricaud, A., 2011. Seasonal variability in the light absorption properties of western Arctic waters: parameterization of the individual components of absorption for ocean color applications. J. Geophys. Res.-Oceans 116.

Merico, A., Tyrrell, T., Brown, C.W., Groom, S.B., Miller, P.I., 2003. Analysis of satellite imagery for Emiliania huxleyi blooms in the Bering Sea before 1997. Geophys. Res. Lett. 30.

Mitchell, B.G., Kahru, M., Wieland, J., Stramska, M., 2002. Determination of spectral absorption coefficients of particles, dissolved material and phytoplankton for discrete water samples. In: Mueller, J.L., Fargion, G.S. (Eds.), Ocean optics protocols for satellite ocean color sensor validation. Revision 3. NASA Technical Memorandum, 2002-21004/Rev3. NASA Goddard Space Center Greenbelt, Maryland, pp. 231–257.

Mopper, K., Kieber, D.J., 2002. Photochemistry and the cycling of carbon, sulfur, nitrogen, and phosphorus. In: Hansell, D.A., Carlson, C.A. (Eds.), Biogeochemistry of Marine Dissolved Organic Matter. Academic Press, pp. 456–489.

Nelson, J.R., Guarda, S., 1995. Particulate and dissolved spectral absorption on the continental-shelf of the southeastern United-States. J. Geophys. Res.-Oceans 100, 8715–8732.

Nelson, N.B., Siegel, D.A., 2002. Chromophoric DOM in the open ocean. In: Hansell, D.A., Carlson, C.A. (Eds.), Biogeochemistry of Marine Dissolved Organic Matter. Elsevier Science, San Diego, pp. 547–578.

Nelson, N.B., Siegel, D.A., Michaels, A.F., 1998. Seasonal dynamics of colored dissolved material in the Sargasso Sea. Deep-Sea Res. I Oceanogr. Res. Pap. 45, 931–957.

Osburn, C.L., Retamal, L., Vincent, W.F., 2009. Photoreactivity of chromophoric dissolved organic matter transported by the Mackenzie River to the Beaufort Sea. Mar. Chem. 115, 10–20.

Pegau, W.S., 2002. Inherent optical properties of the central Arctic surface waters. J. Geophys. Res.-Oceans 107.

Pegau, W.S., Zaneveld, J.R.V., 1993. Temperature-dependent absorption of water in the red and near-infrared portions of the spectrum. Limnol. Oceanogr. 38, 188–192.

Pope, R.M., Fry, E.S., 1997. Absorption spectrum (380–700 nm) of pure water.2. Integrating cavity measurements. Appl. Opt. 36, 8710–8723.

Scully, N.M., Miller, W.L., 2000. Spatial and temporal dynamics of colored dissolved organic matter in the North Water Polynya. Geophys. Res. Lett. 27, 1009–1011.

Siegel, D.A., Maritorena, S., Nelson, N.B., Hansell, D.A., Lorenzi-Kayser, M., 2002. Global distribution and dynamics of colored dissolved and detrital organic materials. J. Geophys. Res. 107, 3228.

Smyth, T.J., Tyrrell, T., Tarrant, B., 2004. Time series of coccolithophore activity in the Barents Sea, from twenty years of satellite imagery. Geophys. Res. Lett. 31, 1–4.

Stedmon, C.A., Markager, S., 2001. The optics of chromophoric dissolved organic matter (CDOM) in the Greenland Sea: an algorithm for differentiation between marine and terrestrially derived organic matter. Limnol. Oceanogr. 46, 2087–2093.

Stedmon, C.A., Markager, S., Kaas, H., 2000. Optical properties and signatures of chromophoric dissolved organic matter (CDOM) in Danish coastal waters. Estuarine Coastal Shelf Sci. 51, 267–278.

Stedmon, C.A., Osburn, C.L., Kragh, T., 2010. Tracing water mass mixing in the Baltic–North Sea transition zone using the optical properties of coloured dissolved organic matter. Estuarine Coastal Shelf Sci. 87, 156–162.

Stedmon, C.A., Amon, R.M.W., Rinehart, A.J., Walker, S.A., 2011. The supply and characteristics of colored dissolved organic matter (CDOM) in the Arctic Ocean: Pan Arctic trends and differences. Mar. Chem. 124, 108–118.

Sturluson, M., Nielsen, T.G., Wassmann, P., 2008. Bacterial abundance, biomass and production during spring blooms in the northern Barents Sea. Deep-Sea Res. II Top. Stud. Oceanogr. 55, 2186–2198.

Våge, S., Basedow, S.L., Zhou, M., Tande, K.S., this issue. Physical structure of the Barents Sea Polar Front near Storbanken in August 2007. J. Mar. Syst.

Vodacek, A., Blough, N.V., DeGrandpre, M.D., Peltzer, E.T., Nelson, R.K., 1997. Seasonal variation of CDOM and DOC in the Middle Atlantic Bight: terrestrial inputs and photooxidation. Limnol. Oceanogr. 42, 674–686.